Title

The Effect of Steady Winds on Radon Entry into Houses

Authors

Riley, W J
Gadgil, A J
Bonnefous, Y C
et al.

Publication Date

1994-10-01

LBL-36372
UC-261
Preprint

Lawrence Berkeley Laboratory

UNIVERSITY OF CALIFORNIA

ENERGY & ENVIRONMENT DIVISION

Submitted to Atmospheric Environment

The Effect of Steady Winds on Radon Entry into Houses

W.J. Riley, A.J. Gadgil, Y.C. Bonnefous, and W.W. Nazaroff

October 1994

ENERGY & ENVIRONMENT DIVISION

Prepared for the U.S. Department of Energy under Contract Number DE-AC03-76SF00098

DISCLAIMER

Submitted to Atmospheric Environment

LBL-36372
UC-261

THE EFFECT OF STEADY WINDS ON RADON ENTRY INTO HOUSES

W. J. Riley[†‡], A. J. Gadgil[†•], Y. C. Bonnefous*, W. W. Nazaroff[‡]

‡ Civil Engineering Department
University of California
Berkeley, CA 94720

† Indoor Environment Program
Lawrence Berkeley Laboratory
Berkeley, CA 94720

*Groupe Informatique et Systemes Energetiques
Ecole Nationale des Ponts et Chaussees
Central 2, La Courtine
93167 Noisy-Le-Grand Cedex
France

October 1994

This work was supported by the Assistant Secretary for Conservation and Renewable Energy, Office of Building Technologies, Building Systems and Materials Division and by the Director, Office of Energy, Office of Health and Environmental Research, Human Health and Assessments Division and Pollutant Characterization and Safety Research Division of the U.S. Department of Energy under Contract No. DE-AC03-76SF00098. Additional support was provided by the National Science Foundation through grant BCS-9057298. The authors wish to thank Bill Fisk for many helpful conversations. Also, the authors wish to thank Phil Price, Ken Revzan, and Rich Sextro for their thorough review of the manuscript.

ABSTRACT

Wind affects the radon entry rate from soil into buildings and the resulting indoor concentration. To investigate this phenomenon, we employ a previously tested three-dimensional numerical model of soil-gas flow around houses, a commercial computational fluid dynamics code, an established model for determining ventilation rates in the presence of wind, and new wind tunnel results for the ground-surface pressure field caused by wind. These tools and data, applied under steady-state conditions to a prototypical residential building, allow us to (1) determine the complex soil-gas flow patterns that result from the presence of wind-generated ground-surface pressures, (2) evaluate the effect of these flows on the radon concentration in the soil, and (3) calculate the effect of wind on the radon entry rate and indoor concentration. For a broad range of soil permeabilities, two wind speeds, and two wind directions, we quantify the "flushing" effect of wind on the radon in the soil surrounding a house, and the consequent sharp decrease in radon entry rates. Experimental measurements of the time-dependent radon concentration in soil gas beneath houses confirm the existence of wind-induced flushing. Comparisons are made to modeling predictions obtained while ignoring the effect of the wind-generated ground-surface pressures. These investigations lead to the conclusion that wind-generated ground-surface pressures play a significant role in determining radon entry rates into residential buildings.

Key word index: radon, wind, indoor air quality, contaminant transport, soil-gas transport

NOMENCLATURE

A_i	cross-sectional area of a portion of the footer-slab crack (m^2)
A_l	effective leakage area (m^2)
A_w	surface-area element of the house's exterior wall (m^2)
$c_p(x,y)$	ground-surface pressure coefficient at location (x,y) (-)
c	Forchheimer term ($s\ m^{-1}$)
C	radon soil-gas concentration ($Bq\ m^{-3}$)
C_{in}	indoor radon concentration normalized with respect to C_∞ (-)
C_{char}	spatial average of the radon soil-gas concentration normalized with respect to C_∞ (-)
C_∞	deep-soil radon concentration ($Bq\ m^{-3}$)
D	diffusivity of radon through bulk soil ($m^2\ s^{-1}$)
D_w	product of the average wall permeability times the area of the wall ($m^3\ s^{-1}\ Pa^{-n}$)
E	normalized radon entry rate into the basement ($m^3\ s^{-1}$)
f_w	local terrain constant (-)
k	soil permeability (m^2)
n	flow exponent (-)
p	disturbance pressure (Pa)
$p_{gs}(x,y)$	ground-surface pressure at location (x,y) (Pa)
p_∞	free-stream air pressure (Pa)
p_i	pressure inside the building (Pa)
p_w	exterior pressure on an element of the house wall (Pa)
ΔP	pressure difference across a section of the house wall (Pa)
Q	ventilation flow rate ($m^3\ s^{-1}$)
Q_i	air flow rate into or out of the building through a section of the exterior wall ($m^3\ s^{-1}$)

Q_{sg}	soil-gas flow rate into the house ($m^3\ s^{-1}$)
$Q_{s,uv}$	ventilation flow from the stack effect and unbalanced ventilation ($m^3\ s^{-1}$)
S	production rate of radon in the soil gas ($Bq\ m^{-3}\ s^{-1}$)
V_{eh}	wind speed at eave height ($m\ s^{-1}$)
$\vec{v}$	soil-gas velocity vector ($m\ s^{-1}$)
α	empirically determined constant used in the footer-slab crack model ($m^3\ s\ kg^{-1}$)
β	empirically determined constant used in the footer-slab crack model ($s\ m^{-1}$)
ε	porosity of the soil (-)
λ	radon decay constant (s^{-1})
μ	dynamic viscosity of air ($kg\ m^{-1}\ s^{-1}$)
ρ	air density ($kg\ m^{-3}$)

INTRODUCTION

The recognition that indoor radon is a serious health concern has resulted in a substantial effort to elucidate the factors that determine both its entry rate into buildings and its indoor concentrations. Detailed studies, both experimental and numerical, have investigated the effects of environmental conditions, building characteristics (such as the presence of a basement or crawlspace), and the operation of mechanical ventilation systems and furnaces on radon entry into buildings. Insights from this research have led to numerical models designed to predict radon entry rates into buildings for simple, well characterized soils, and under relatively stable meteorological conditions.

Advective entry of radon-bearing soil gas is the dominant source of indoor radon in most homes with elevated concentrations (Nazaroff, 1992). In buildings with basements, a small depressurization is sufficient to drive soil gas through cracks in the substructure (such as the joints between the footer and basement slab running along the periphery of the basement). The driving force for this entry is the small indoor-outdoor pressure difference (on the order of one to ten Pa) which can be generated by indoor-outdoor temperature differences, space conditioning equipment, mechanical exhaust, and the interaction of wind with the building structure. Among these, wind is unique since, in addition to depressurizing the building, it alters the pressure on the ground-surface adjacent to the building. This wind-induced ground-surface pressure field influences soil-gas flow thereby altering the radon concentration in the soil gas surrounding the building. As summarized below, evidence suggesting that wind can play a role in determining the amount of radon that enters a house has been presented elsewhere. Little has been published, however, with the intent of quantifying this role and understanding the mechanisms involved.

Passive or low-energy radon mitigation systems can also be influenced by wind (Fisk et al., 1994). The effects are especially pronounced when a direct connection between the atmosphere and sub-slab gravel layer is present. Design of these systems will need to account for both the effect of wind on soil-gas concentrations and on the method of coupling the gravel layer to the outdoors.

A striking example of the effects of wind on radon entry rates and indoor concentrations was presented by Turk et al. (1990). Figure 1 reproduces their data for a house in the Pacific Northwest showing a strong inverse correlation between wind speed and indoor radon concentration. Although some

of the decrease in the indoor radon concentration with increasing wind speed is due to increased ventilation, this factor is not large enough to account for the full reduction shown. A concurrent reduction in the radon entry rate must also have occurred. The authors hypothesized that the wind ventilated the soil surrounding the house, thus reducing the soil-gas radon available for entry into the building. In the *Results* section of this paper we present direct experimental evidence of soil-gas flushing at several test houses in New Jersey, and indicate that this depletion follows the trends predicted in our numerical simulations.

Nazaroff et al. (1985) instrumented a house in Illinois to monitor the effects of various environmental factors on radon entry rates. They concluded that when the indoor-outdoor temperature difference was small, high wind speeds were associated with higher radon entry rates, and conversely, when this temperature difference was large, low wind speeds produced higher radon entry rates. They also noticed a correlation between high wind speeds and decreased radon concentrations in the soil gas, possibly as a result of the flushing of radon from the soil gas. Their observations did not lead to conclusive elucidation of the mechanisms responsible for these relationships.

Arnold (1990) conducted an experiment with a three-dimensional scale model of a house, and imposed on the ground surface a simplified version of the wind-induced ground-surface pressure distribution reported by Scott (1985). Resulting perturbations of the pressure field in the porous medium used to represent the soil were then measured. However, radon concentrations in the ersatz soil were not measured, and therefore the effect of wind on radon entry rates into the basement was not determined. Ward et al. (1993), in their experimental study of a small building structure, observed a correlation between wind speed and the pressure difference between indoor air and the soil gas. However, the above-ground structure in these experiments is not geometrically similar to a real house. It is therefore difficult to extend these correlations to full scale houses, which are affected by both wind-induced depressurization and the ground-surface pressure field.

Scott (1985) reported a numerical investigation of the effects of wind speed and direction on radon entry rates using a finite-element model of a simple building. Ground pressure data generated in a small wind tunnel and meteorological data from a summer and winter period in Toronto were used as

input to the simulations. Their simulations predicted that both wind speed and wind direction affect the radon entry rate into a building, but they found no simple correlation among these factors. Sherman (1992) developed a simplified model of a house to quantify the effects of several factors, including wind, on radon entry. Sherman assumed that the wind did not deplete the soil gas of radon, but did increase the ventilation rate and basement depressurization. He concluded that the stack effect is much more effective at inducing radon entry than is the wind effect. Owczarski et al. (1991) performed a numerical study of the effects of wind and reported expected reductions in the soil-gas radon concentration below a slab-on-grade house. However, the study ignores crucial details of building structure (e.g., existence of footers), does not consider the full two-dimensional nature of the wind-generated ground-surface pressure field, uses arbitrary values for wind-generated ground-surface pressures, and considers only Darcy flow through the soil and gravel layer.

Taken in combination, these efforts do not yield a comprehensive picture of how wind affects radon entry rates and indoor concentrations. We aim to improve our understanding by reporting on a detailed investigation of wind-induced radon entry into a prototypical residential building under steady-state conditions. This study particularly emphasizes two issues: the effect of wind-induced ground-surface pressures on the soil-gas radon concentration near a house, and the interplay between ventilation and radon entry in affecting indoor concentrations when both are driven by wind. To pursue these objectives, we employ a largely numerical approach, combining three modeling tools with new wind tunnel data of the ground-surface pressure field induced by wind blowing on a building. The modeling tools comprise (1) a previously tested, three-dimensional finite-difference model, known as Non-Darcy STAR, of soil-gas flow and radon concentrations around buildings (Gadgil et al., 1991, Bonnefous et al., 1992); (2) a commercial computational fluid dynamics code, FLUENT (FLUENT, 1993); and (3) a model for determining the house ventilation rate in the presence of wind (Sherman, 1992). We also present previously acquired but unpublished experimental data that qualitatively substantiates key model predictions.

METHODS

Overview

The simulation of the wind's interaction with the building and surrounding soil was carried out in a five-step process. First, results from recent wind tunnel experiments were used to compute the wind-generated ground-surface pressure field around the house. Second, the wind-induced depressurization in the house was calculated from FLUENT's predictions of the distribution of pressures on the exposed walls. Third, the pressure and velocity fields in the soil gas surrounding the house and in the sub-slab gravel layer were computed using Non-Darcy STAR. Fourth, the soil-gas radon concentration field was determined and a radon entry rate into the house was calculated. Finally, the indoor radon concentration was computed using a predicted wind-induced enhancement of the building's ventilation rate. This five-step exercise, which is described in more detail below, was carried out for a range of soil permeabilities, two wind speeds, and two wind directions.

A central approximation in this study is that wind establishes a steady-state ground-surface pressure field, depressurization of the house, and flow of soil gas and radon. In reality, both wind speed and direction vary with time. Over the range of soil permeabilities we will consider, the soil-gas pressure field will reach a steady state after a perturbation with a characteristic time of seconds to minutes (Nazaroff et al., 1988). The soil-gas concentration field will reach a steady state with a characteristic time that is the smaller of 1) the time soil gas takes to travel from the soil surface to the basement (on the order of hours to months, depending on the soil permeability), and 2) the time required for the radon concentration to reach a steady value as a result of its radioactive generation and decay (several days).

Macrometeorological wind fluctuations typically have peaks in the wind energy distribution at periods on the order of days. In contrast, small scale wind fluctuations have significant energy at periods on the order of a minute (Van der Hoven, 1957). For the macrometeorological region of the wind spectrum, the soil-gas pressure field is likely to reach steady state. However, because the time required for the radon concentration field to equilibrate can be large, the assumption of a steady soil-gas concentration field is not strictly appropriate, even for large scale wind fluctuations. Still, the assumption of steady state

captures some of the key features of the problem, and is therefore useful as an important step towards understanding the effects of wind on radon entry into homes.

House substructure and soil characteristics

The house geometry was chosen to represent a typical single-family structure in size and aspect ratio, but not intended to characterize a statistically "normal" home. The building has a plan area of 8.7 m x 10.4 m; the basement and footers represent standard construction practice and are depicted in Figure 2 (a). A 1 mm L-shaped crack provides the route for advective entry of radon into the basement. Advective flow through this channel is modeled with the equation (Baker et al., 1987)

$$\vec{\nabla} p = \alpha(1+\beta|\vec{v}|)\vec{v} \qquad (1)$$

where p is the disturbance pressure (Pa), α and β are empirically determined constants that are functions of the crack geometry, and $\vec{v}$ is the soil-gas velocity vector (m s^{-1}). For this study α is 1.2×10^{-3} m^3 s kg^{-1} and β is 0.035 s m^{-1} (Gadgil et al., 1991).

We varied the permeability of the soil surrounding the house from 1×10^{-11} m^2 to 1×10^{-8} m^2. The lower bound was chosen because wind does not significantly affect soil-gas radon concentrations below this value. The upper bound is a permeability above which no houses are expected to be found (Nazaroff, 1992). The permeability of the gravel placed under the basement slab is taken as 3×10^{-7} m^2, corresponding approximately to a 4.5 cm round gravel (Gadgil et al., 1991).

Wind-Induced Ground-Surface Pressure Field

The pressure field established around a house in the presence of wind was determined by conducting scale experiments in the U.C. Berkeley Architecture Department's wind tunnel facility (see Bauman et al., 1988, for a description of the wind tunnel, and Riley et al., 1994, for details regarding these experiments). For the results presented here, the house is a box of dimension 8.7 m x 10.4 m x 3 m. The ground-surface pressure coefficient, $c_p(x, y)$, is defined as

$$c_p(x,y) = \frac{p_{gs}(x,y) - p_\infty}{\frac{1}{2}\rho V_{eh}^2} \qquad (3)$$

where $p_{gs}(x,y)$ is the ground-surface pressure (Pa) at location (x,y), p_∞ is the free-stream pressure (Pa), ρ is the air density (kg m^{-3}), and V_{eh} is the free-stream wind speed at eave height (m s^{-1}). Figures 3 (a) and 3 (b) present the ground-surface pressure coefficient field for the case of wind incident perpendicular to the short side of the house and incident at 45° to the side of the house, respectively.

Eave-height wind speeds of 0, 3.6, and 8.3 m s^{-1} are used in combination with equation (3) and the results presented in Figure 3 to define the ground-surface pressure field for the simulations. The non-zero wind speeds correspond to the 5th and 95th percentile wind speeds, respectively, over a period of approximately 25 years in Spokane, Washington (NOAA, 1980). This location was chosen because radon entry and mitigation has been investigated in several houses in the area (Turk et al., 1990). For comparison, the average wind speed in the U.S. is 4.1 m s^{-1}.

Wind-Induced Indoor Depressurization

The depressurization of the house air can be caused by several factors. We consider only wind-induced depressurization in order to focus attention on the effects of wind on the radon entry rate. Physically, this situation would occur under steady wind conditions when the indoor-outdoor temperature difference is small and no mechanical ventilation or heating equipment is operating. To highlight the importance of including the wind-induced ground-surface pressures, we have performed analogous simulations (same house geometry and range of soil permeabilities) with the ground surface at atmospheric pressure and a basement depressurization of -10.6 Pa. This is the basement depressurization that we estimate is caused by an 8.3 m s^{-1} wind, as described below.

The indoor depressurization is computed by balancing the total flow into and out of the building (Mowris and Fisk, 1988)

$$Q_i = D_w(\Delta P)^n \tag{4}$$

where Q_i is the air flow rate into or out of the building through the section of the exterior wall being considered ($m^3\ s^{-1}$), D_w is the product of the average wall permeability times the area of that section of the wall ($m^3\ s^{-1}\ Pa^{-n}$), ΔP is the pressure difference across that section of the wall (Pa), and n is a flow exponent (-). The flow exponent depends on the character of the flow through the cracks: it is 1.0 for flow dominated by viscous forces, and 0.5 for flow dominated by inertial forces. A typical value, integrated over all the cracks in a house, is 0.66 (Sherman, 1984). By assuming an equal distribution of leakage area around the house, the flow balance for a building with no mechanical supply or exhaust can be written as

$$\sum_{surfaces}(A_w)*\text{sign}(p_w - p_i)*(p_w - p_i)^n = 0 \tag{5}$$

where A_w is a surface-area element of the exterior wall (m^2), p_w is the exterior pressure on an element of the house wall (Pa), and p_i is the pressure inside the building (Pa).

We used FLUENT to determine p_w by solving the conservation equations for mass and momentum in the air flow around the house. FLUENT discretizes the space with a control-volume based, finite-difference technique, and we used the k-ε model to simulate turbulence. The computational grid included open space a distance of six house dimensions from the building in both horizontal directions, a vertical dimension of 61 m, and was divided into 100,000 control volumes. The building's walls were modeled as smooth surfaces. We have assumed that the house is isolated from other buildings, and that the atmospheric boundary layer corresponds to what might be expected on the outskirts of a small town (see Riley et al., 1994, for details of this simulation).

Equation (5) is solved iteratively once the values for p_w are determined. With the wind perpendicular to the short side of the house, the interior depressurization is predicted to be -10.6 Pa for a wind speed of 8.3 m s^{-1}, and -2.00 Pa for a wind speed of 3.6 m s^{-1}.

The predicted values of p_i are subject to inaccuracies inherent in the FLUENT simulation. Therefore, we also computed the building depressurization by the method of Feustel (1985) to obtain an indication of the uncertainty in p_i. This technique uses average wall surface pressure coefficients to compute the basement depressurization as a function of the eave-height free-stream dynamic pressure. With the wind perpendicular to the short side of the house, the indoor depressurization is predicted to be -12.5 Pa for a wind speed of 8.3 m s^{-1}, and -2.35 Pa for a wind speed of 3.6 m s^{-1}. These values are both within 20% of the values calculated using FLUENT.

Soil-gas Pressure and Velocity Fields

The soil-gas pressure, velocity, and concentration fields were computed in a soil block that measures 30.4 m x 26.2 m horizontally, and extends 11.9 m below the soil surface (Figure 2 (b)). There are 40,716 node points in this volume. The exterior surfaces of the soil block are taken to be Neumann boundaries (no flow), as are all interfaces where the soil meets the basement. The Neumann boundary at the bottom of the computational space is equivalent to assuming that an impermeable layer exists at this depth (e.g., water table). Dirichlet boundaries (fixed pressure) are imposed on the ground surface and along the crack that connects the sub-slab gravel layer with the basement.

The pressure and velocity fields in the soil gas are solved simultaneously using a three-dimensional finite-difference software package called Non-Darcy STAR (Gadgil et al., 1991, Bonnefous et al., 1992). This package can model both Darcy and non-Darcy flow of soil gas, as appropriate, in regions of gravel and soil. The non-Darcy flow is modeled with the Darcy-Forchheimer equation:

$$\vec{\nabla} p = -\frac{k}{\mu}(1 + c|\vec{v}|)\vec{v} \qquad (8)$$

where p is the soil-gas disturbance pressure (Pa), k is the soil permeability (m^2), μ is the dynamic viscosity (kg m^{-1} s^{-1}), and c is the Forchheimer term (s m^{-1}). Gadgil et al. (1991) describe the experimental procedure used to determine the Forchheimer term.

Since the disturbance pressure is always small relative to atmospheric pressure, the soil gas is treated as incompressible. Therefore, the continuity equation becomes:

$$\vec{\nabla} \cdot \vec{v} = 0 \tag{9}$$

The model assumes that each zone of soil is homogeneous and isotropic, the concrete basement walls and floor are impermeable to soil-gas flow (except through the cracks), and the effect of buoyancy on soil-gas flow is negligible. A modified SIMPLE algorithm (Patankar, 1980) is used to discretize equations (8) and (9), and the pressure and velocity fields are calculated on staggered grids using an alternate direction implicit method. The solution procedure is considered adequately converged when the computed pressure at each point changes by less than 1×10^{-6} over successive iterations.

Soil-Gas Concentration Field

Given the soil-gas velocity field, the radon concentration is calculated from the steady-state radon mass balance equation

$$\vec{\nabla} \cdot \left(D \vec{\nabla} C\right) - \vec{\nabla} \cdot (\vec{v} C) + \varepsilon (S - \lambda C) = 0 \tag{10}$$

where C is the radon concentration in the soil gas (Bq m^{-3}), D is the diffusivity of radon through bulk soil (m^2 s^{-1}), S is the production rate of radon into the soil gas (Bq m^{-3} s^{-1}), λ is the radon decay constant (s^{-1}), and ε is the porosity of the soil (-). In contrast to the pressure and velocity field computations, the ground surface here is treated as a mixed boundary condition because there may be areas (i.e. on the leeward side of the house) where the magnitudes of the advective and diffusive radon flux out of the ground are comparable.

The normalized radon entry rate into the basement is then calculated by summing the flux into the crack over the cross-sectional area of the crack

$$E = \frac{\sum_i C \cdot \vec{v} \cdot A_i}{C_\infty} \tag{11}$$

where E is the normalized radon entry rate into the basement ($m^3\ s^{-1}$), A_i is the cross-sectional area (m^2) of the portion of the crack under consideration, C and $\vec{v}$ are evaluated at the opening of the crack in the gravel layer, and C_∞ is the radon concentration in the soil gas far below the surface (Bq m^{-3}).

Indoor Radon Concentration

The normalized, steady-state indoor radon concentration is calculated from the normalized radon entry rate and an estimate of the house's ventilation rate. We use the LBL infiltration model (Sherman, 1992) to estimate the ventilation flow rate, Q ($m^3\ s^{-1}$), in the presence of wind:

$$Q = \left[A_l^{\,2} f_w^{\,2} V_{eh}^{\,2} + Q_{sg}^{\,2} + Q_{s,uv}^{\,2}\right]^{0.5} \tag{12}$$

where A_l is an effective leakage area (m^2), f_w is a wind parameter equal to 0.23, corresponding to a lightly shielded building (Mowris and Fisk, 1988), Q_{sg} is the soil-gas flow rate into the house ($m^3\ s^{-1}$), and $Q_{s,uv}$ is the ventilation flow ($m^3\ s^{-1}$) from the stack effect and unbalanced ventilation. Note that for cases with wind, $Q_{s,uv}$ is set to zero, and for cases without wind, V_{eh} is set to zero. We use an effective leakage area of 6.1×10^{-2} m^2. This number was reported by Palmiter and Brown (1989) in their study of Northwest houses as an average value for homes without ducted heating systems.

Table 1 lists the four simulation cases we examined and indicates for each the basement depressurization, house air exchange rate, and whether wind-induced ground-surface pressures are included.

The normalized indoor radon concentration, C_{in}, is calculated as

$$C_{in} = \frac{E}{Q} \tag{13}$$

The dimensional indoor radon concentration equals the product of C_{in} and C_∞. A typical value for C_∞ is 30 kBq m^{-3} (Nazaroff, 1992).

RESULTS AND DISCUSSION

Radon and Soil-Gas Entry Rates

Figure 4 (b) shows predicted normalized radon entry rates as a function of soil permeability for wind speeds of 3.6 and 8.3 m s^{-1} at a wind incidence angle of 0°, and for a wind speed of 8.3 m s^{-1} at a wind incidence angle of 45°. We plot the results for case 1 on a separate graph (Figure 4 (a)) to emphasize that here the ground surface is at atmospheric pressure, although the basement depressurization remains -10.6 Pa.

The simulation predictions for case 1 follow a commonly observed pattern over a wide range of house geometries (e.g., Revzan and Fisk, 1992). For soil permeabilities less than about $1x10^{-10}$ m^2 the radon entry rate increases linearly as soil permeability increases. However, as the soil permeability increases above this value, the radon entry rate begins to level off. The lower resistance to soil-gas flow accompanying the increase in soil permeability causes more of the pressure drop between the basement and the soil surface to occur across the footer-slab crack. The result is a lower driving force for soil-gas movement and hence radon entry. For larger crack sizes, the flow of soil gas into the basement can continue to increase with increasing soil permeability (Mowris and Fisk, 1988). In this case, the radon depletion in the soil gas adjacent to the crack can also be a factor in limiting the radon entry rate at high soil permeabilities.

The simulation predictions for cases 2, 3, and 4 show a remarkably different dependence on soil permeability. For the lower wind speed, the radon entry rate peaks at a soil permeability of about $3x10^{-10}$ m^2; further increases in soil permeability lead to sharply lower radon entry rates. At the higher wind speed, the radon entry rate declines continuously as the soil permeability increases.

Simulations were also performed with the higher basement depressurizations computed using the technique of Feustel (1985): -12.5 Pa for a wind speed of 8.3 m s^{-1} and -2.35 Pa for a wind speed of 3.6 m s^{-1}. The shape of the curves were similar to those shown in Figure 4, demonstrating that the qualitative effect of wind on the radon entry rate is not a sensitive function of this parameter.

The predicted soil-gas flow rate into the basement is shown in Figure 5 (a) for case 1, and Figure 5 (b) for cases 2, 3, and 4. For soil permeabilities larger than $3x10^{-11}$ m^2, the flow rate is predicted to be less when the wind is blowing than when it is not. Wind pressurizes one side and depressurizes three sides of the building with respect to the free-stream pressure. This effect reduces the soil-gas entry rate because the net area-weighted pressure difference between the basement and the ground surface is reduced. However, the trend of the soil-gas entry rate versus soil permeability curve is similar to the case without wind.

Wind-Induced Flushing of Soil-Gas Radon

A detailed examination of the simulation results shows the underlying reason for the sharp drop in radon entry rate with increasing soil permeability when the house is exposed to wind. The bulk soil-gas flow under the house that is driven by wind-induced ground-surface pressures increases dramatically as the soil permeability increases. In this flow, air enters the ground on the windward side of the house, and soil gas exits the ground surface on the other three sides of the building. The result is a significant flushing of radon from the soil gas beneath the house, and as a consequence, a diminished source for radon entry into the basement. In addition, because of the complex distribution of pressure on the ground surface there are unanticipated soil-gas flow patterns on the leeward side of the house.

Figure 6 (a) shows normalized soil-gas radon concentrations in a vertical plane bisecting the soil block parallel to both the long side of the house and an 8.3 m s^{-1} wind. The dominant flow paths for the soil gas (not shown in Figure 6) start from the soil surface on the left, proceed under the house, and exit from the soil surface on the right. For comparison, Figure 6 (b) shows the analogous contours of soil-gas radon concentration for the case without wind. The extent to which the wind flushes radon from the soil gas is illustrated by comparing Figures 6 (a) and 6 (b). It is apparent that increasing soil permeability in the presence of wind leads to sharply depressed levels of soil-gas radon in the vicinity of the footer-slab crack.

To quantify this effect, we define a characteristic soil-gas radon concentration, C_{char}, to represent the radon source available for entry into the basement. C_{char} is calculated by taking the area-weighted average of the radon concentration in a plane surface bounded by the lower interior edges of the footers. Figure 7 presents this parameter for the same four cases considered in Figure 4. When there is no wind, C_{char} is not a sensitive function of soil permeability (Figure 7 (a)), and the result is a radon entry rate that generally follows the soil-gas flow rate into the basement (compare Figures 4 (a) and 5 (a)). However, in the presence of wind, C_{char} decreases sharply with increasing soil permeability (Figure 7 (b)), leading to a decreasing radon entry rate (compare Figures 4 (b) and 5 (b)). To summarize, the higher the soil permeability, the larger the extent of soil-gas flushing in the presence of a steady wind. The result is a lower available radon source, and therefore a lower radon entry rate.

Figure 8 shows soil-gas streamlines for an 8.3 m s^{-1} wind and a soil permeability of 3×10^{-9} m^2 in the same vertical plane used in Figure 6. Notice the significant flow of soil gas that enters the gravel layer on the windward side of the house, moves through the gravel layer, and then exits on the leeward side. The high permeability gravel layer offers a preferred short-circuit path between the windward and leeward sides of the house. The second interesting (and unexpected) feature of the flow occurs in the soil region on the leeward side of the house, where soil gas is moving back toward the house. This peculiarity results because the leeward ground-surface pressure far from the house is larger than the pressure near the house (see Figure 3 (a)). Although the magnitude of the flow depends on soil permeability, the qualitative features shown here are fairly constant over the range of soil permeabilities and wind speeds examined.

Indoor Radon Concentration

The calculated indoor radon concentration, C_{in}, is plotted as a function of wind speed and soil permeability in Figure 9. Notice that the indoor radon concentration curves are similar in form to the radon entry rate curves shown in Figure 4. Figures 4 and 9 suggest that a house exposed to a sustained wind will experience a substantial decrease in radon entry rate and indoor concentration, and that this

decrease is a result not only of the increase in ventilation associated with the wind, but of the concurrent flushing of radon from the soil gas in the vicinity of the house.

Experimental Evidence of Soil-Gas Flushing

One of the key predictions of our model is that the radon concentration in soil gas near a house can be depleted by wind-induced flushing. To explore whether this predicted behavior occurs in reality, we examined previously acquired data from a study of radon entry and mitigation in New Jersey (Turk et al., 1991). In this study, seven houses were instrumented to determine the effectiveness of five different radon control techniques. For several of these houses, control periods occurred during which no mitigation system was operating and indoor and outdoor temperatures, sub-slab soil-gas radon concentrations, and wind speeds were monitored simultaneously. The sub-slab radon measurements were taken approximately in the center of the slab near the interface between the gravel and soil. We examined the data from three houses: LBL09, LBL10, and LBL14. Ten periods were identified during which the wind speed was low for several hours, then increased and remained high for several hours, and the indoor-outdoor temperature difference was relatively stable. The change in soil-gas radon concentration over each of these periods was determined. For nine of the ten periods the soil-gas radon concentration was observed to diminish in response to increasing wind. Figure 10 shows two periods from one house that are illustrative of the effects of wind on the soil-gas radon concentration. Table 2 presents the wind speeds and soil-gas radon concentrations (computed as a two-hour average) immediately before (low wind) and during (high wind) the ten episodes in the three houses.

Several assumptions employed in the model calculations are not met in these experiments: steady wind speed and direction, steady indoor-outdoor temperature difference, and a wind direction of 0 or 45°. In addition, the modeled house geometry is different than all three of these houses, and the soil-gas radon concentrations and small-scale soil permeability measurements are from only one or two locations near the house. Therefore, these experiments cannot be used to quantitatively validate our modeling results.

They do, however, support a key qualitative finding, that wind reduces soil-gas radon concentrations in the vicinity of a house.

CONCLUSIONS

Wind has a significant effect on radon entry rates and indoor concentrations in houses with basements. In addition to the well-established results that wind increases the building's ventilation rate and relative depressurization, soil-gas flow generated by wind-induced ground-surface pressures flushes radon from the soil near the house. The concentration of radon in the soil gas being drawn into the basement is therefore reduced; the result is a substantially lower radon entry rate. Since real houses are regularly exposed to wind, this effect must be included if radon entry is to be properly modeled.

The effect of ignoring wind-induced ground-surface pressures is illustrated by comparing the radon entry rates and indoor concentrations for cases 1 and 2 (Figures 4 and 9). For both of these simulations, the basement depressurization is -10.6 Pa; the difference between them is the inclusion of the ground-surface pressure field for case 2. The radon entry rate and indoor concentration are comparable for the two cases at a soil permeability of 1×10^{-11} m^2. In the absence of wind-induced ground-surface pressures, the radon entry rate and indoor concentration increase by about an order of magnitude as the soil permeability is increased to 1×10^{-8} m^2. In contrast, there is about a two order of magnitude decrease in radon entry rate and indoor concentration in response to the same change in permeability when the ground-surface pressures are included. Therefore, predictions concerning the effect of wind on indoor radon concentrations that ignore ground-surface pressures will be substantially in error, especially in regions having high soil permeability.

In addition to the cases presented here, we have conducted simulations with other ground-surface pressure fields (based on Scott's (1985) wind tunnel results and numerical simulation results from FLUENT), basement depressurizations, wind speeds, and wind angles. The effect of wind on the radon entry rate was found to be qualitatively the same as in the cases summarized here. We therefore conclude that, for this house geometry, the observed trends are robust.

The effect of a time-varying wind velocity on radon entry rates and indoor concentrations remains an unresolved issue. We are currently working to expand the capabilities of our non-Darcy

STAR model to analyze this scenario. Inclusion of time-varying soil-gas pressure, velocity, and concentration fields, in addition to a time-varying basement depressurization, will be necessary. The latter will be a function of both the fluctuating wind and the characteristics of the building shell, which will define how an external pressure is propagated throughout the house. Furthermore, an understanding of the effects of transient winds on radon entry is expected to be important in the design of passive or low-energy mitigation systems where a direct connection between the atmosphere and the sub-slab gravel layer may be present (Fisk et al., 1994).

Further work is also required to determine the effect of wind on the radon entry rate into houses with different geometries (e.g., L-shaped or split-level homes) and high-rise buildings. Such buildings may respond differently than the predictions reported here because of the expected distinctions in the wind-induced ground-surface pressure field.

In summary, we have found the effects of a steady wind on radon entry rates and indoor radon concentrations to be substantial. Accounting only for the increase in building depressurization and ventilation is insufficient to predict the effect of wind on indoor radon concentrations. The concurrent flushing of radon from the soil gas that is driven by wind-generated ground-surface pressures must also be considered. Further study of the effects of wind on radon entry (i.e. considering transient winds and different building geometries) is necessary to complete our understanding of this phenomenon and enable us to design mitigation systems that can most efficiently reduce human exposures.

Acknowledgments-This work was supported by the Assistant Secretary for Conservation and Renewable Energy, Office of Building Technologies, Building Systems and Materials Division and by the Director, Office of Energy, Office of Health and Environmental Research, Human Health and Assessments Division and Pollutant Characterization and Safety Research Division of the U.S. Department of Energy under Contract No. DE-AC03-76SF00098. Additional support was provided by the National Science Foundation through grant BCS-9057298. The authors wish to thank Bill Fisk for many helpful conversations. Also, the authors wish to thank Phil Price, Ken Revzan, and Rich Sextro for their thorough review of the manuscript.

Figure 1. Indoor radon concentration and wind speed measured over a three-week period at ESP111 (Spokane, WA) from the study by Turk, et al. (1990). Note the inverse correlation between wind speed and indoor concentration, and the magnitude of the reduction in indoor concentration during the periods of high wind speeds.

Figure 2. Geometry of the substructure of the house (a) and the computational space (b). The diagrams are not drawn to scale.

Figure 3. Contour plot of the ground-surface pressure coefficient (plan view) for wind incident at an angle of 0° (a) and 45° (b) to the house. The pressure coefficient is the fraction of the eave-height dynamic pressure of the wind that is felt on the ground surface.

Figure 4. Normalized radon entry rate into the basement as a function of soil permeability. The radon entry rate is normalized with respect to the deep-soil radon concentration. The gravel permeability is 3×10^{-7} m^2. The basement depressurization for no wind (i.e., no wind-induced ground-surface pressures) is -10.6 Pa, for the 3.6 m s^{-1} wind it is -2.00 Pa, and for the 8.3 m s^{-1} wind it is -10.6 Pa. Note the different y-axis scales for Figures 4 (a) and 4 (b).

Figure 5. Soil-gas entry rates into the basement as a function of soil permeability. The shape of the curve for no wind (a) is characteristic of a wide range of house geometries. The basement depressurization for no wind (i.e., no wind-induced ground-surface pressures) is -10.6 Pa, for the 3.6 m s^{-1} wind it is -2.00 Pa, and for the 8.3 m s^{-1} wind it is -10.6 Pa.

Figure 6 (a). Contour plots of soil-gas radon concentration at several soil permeabilities for the case of an 8.3 m s^{-1} wind (the concentration is normalized with respect to the deep-soil radon concentration). Figures represent concentrations in a vertical plane bisecting the basement

parallel to the long side of the house and the wind direction. As the soil permeability increases, the radon concentration in the soil gas adjacent to the slab decreases. Note the magnitude of the reduction in soil-gas radon concentration compared to the case with no wind (Figure 6 (b)).

Figure 6 (b). Contour plots of soil-gas radon concentration at several soil permeabilities for the case of no wind (the concentration is normalized with respect to the deep-soil radon concentration). Figures represent concentrations in a vertical plane bisecting the basement parallel to the long side of the house.

Figure 7. Average radon soil-gas concentration (C_{char}) at a horizontal plane located at the bottom of the footers, and bounded by the footers (the concentration is normalized with respect to the deep-soil radon concentration). The basement depressurization for no wind (i.e., no wind-induced ground-surface pressures) is -10.6 Pa, for the 3.6 m s^{-1} wind it is -2.00 Pa, and for the 8.3 m s^{-1} wind it is -10.6 Pa.

Figure 8. Streamlines of soil gas flow in the soil block and in the gravel layer. The wind speed is 8.3 m s^{-1}, the soil permeability is $3x10^{-9}$ m^2, and the gravel permeability is $3x10^{-7}$ m^2.

Figure 9. Normalized indoor radon concentration as a function of wind speed and soil permeability. The basement depressurization for no wind (i.e., no wind-induced ground-surface pressures) is -10.6 Pa, for the 3.6 m s^{-1} wind it is -2.00 Pa, and for the 8.3 m s^{-1} wind it is -10.6 Pa.

Figure 10. Wind speed and soil-gas radon concentration for two time periods at house LBL09 (Morristown, NJ) (Turk et al., 1991). Wind-driven soil-gas flow is flushing radon from the area adjacent to the house.

Table 1. Wind conditions, basement depressurization, and air exchange rate for the four simulation cases.

Table 2. Change in soil-gas radon concentration as a result of wind. Data culled from the LBL study of houses in New Jersey, reported in Turk et al., (1991).

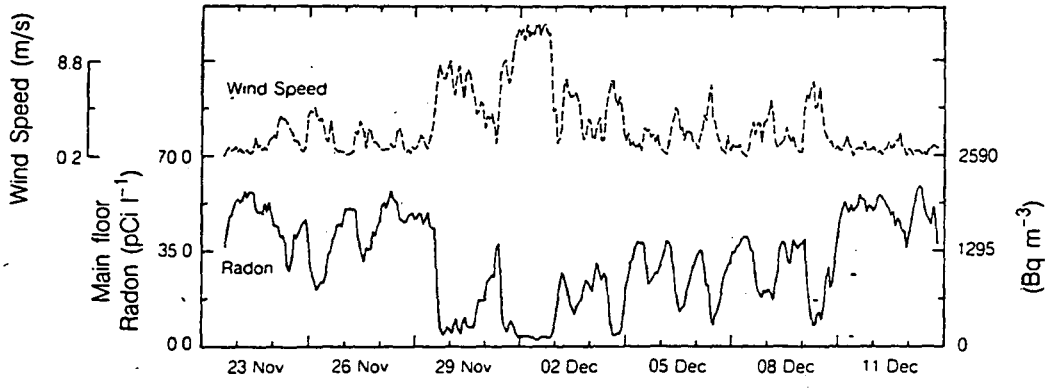
Wind Speed (m/s)
8.8
0.2
Wind Speed
Main floor
Radon (pCi l^{-1})
70.0
35.0
0.0
Radon
2590
1295
0
(Bq m^{-3})
23 Nov
26 Nov
29 Nov
02 Dec
05 Dec
08 Dec
11 Dec

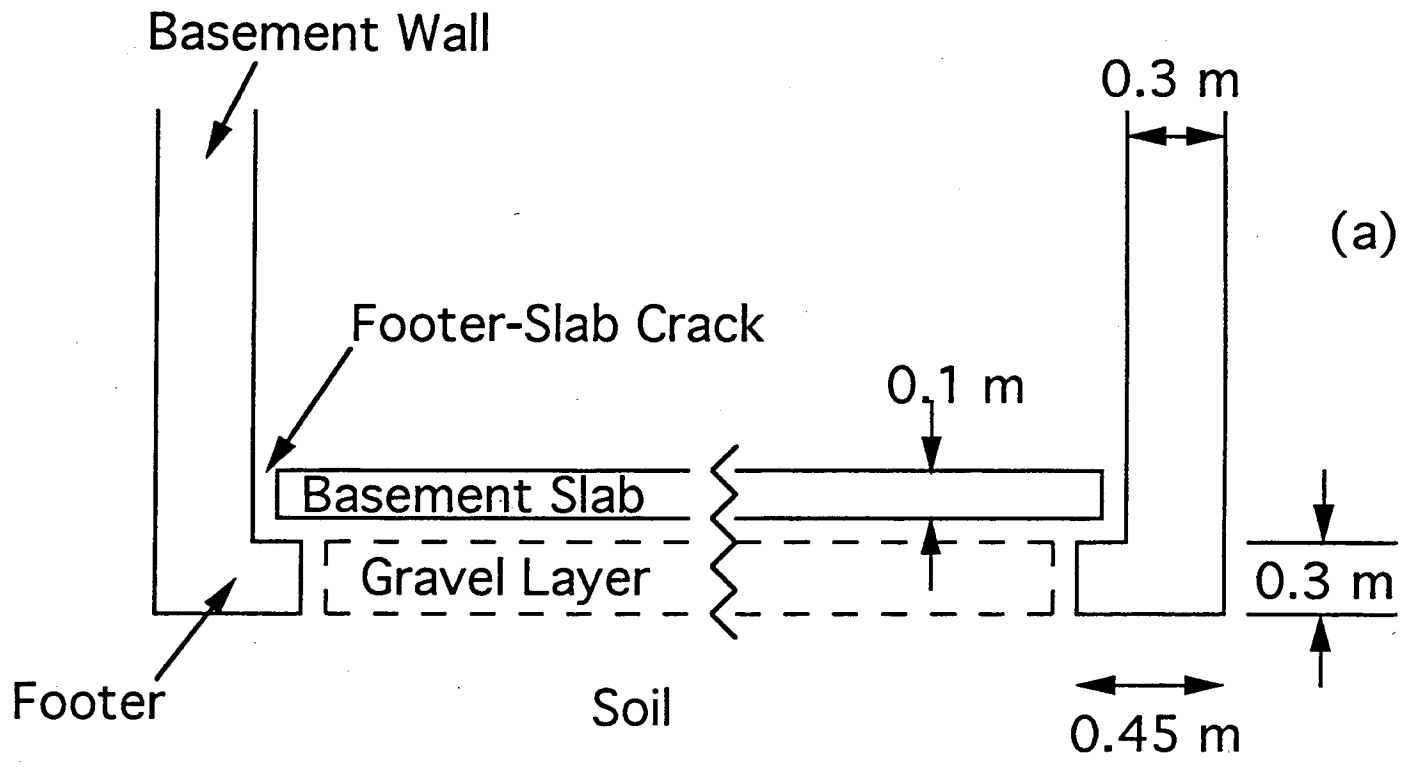
Basement Wall
0.3 m
(a)
Footer-Slab Crack
0.1 m
Basement Slab
Gravel Layer
0.3 m
Footer
Soil
0.45 m

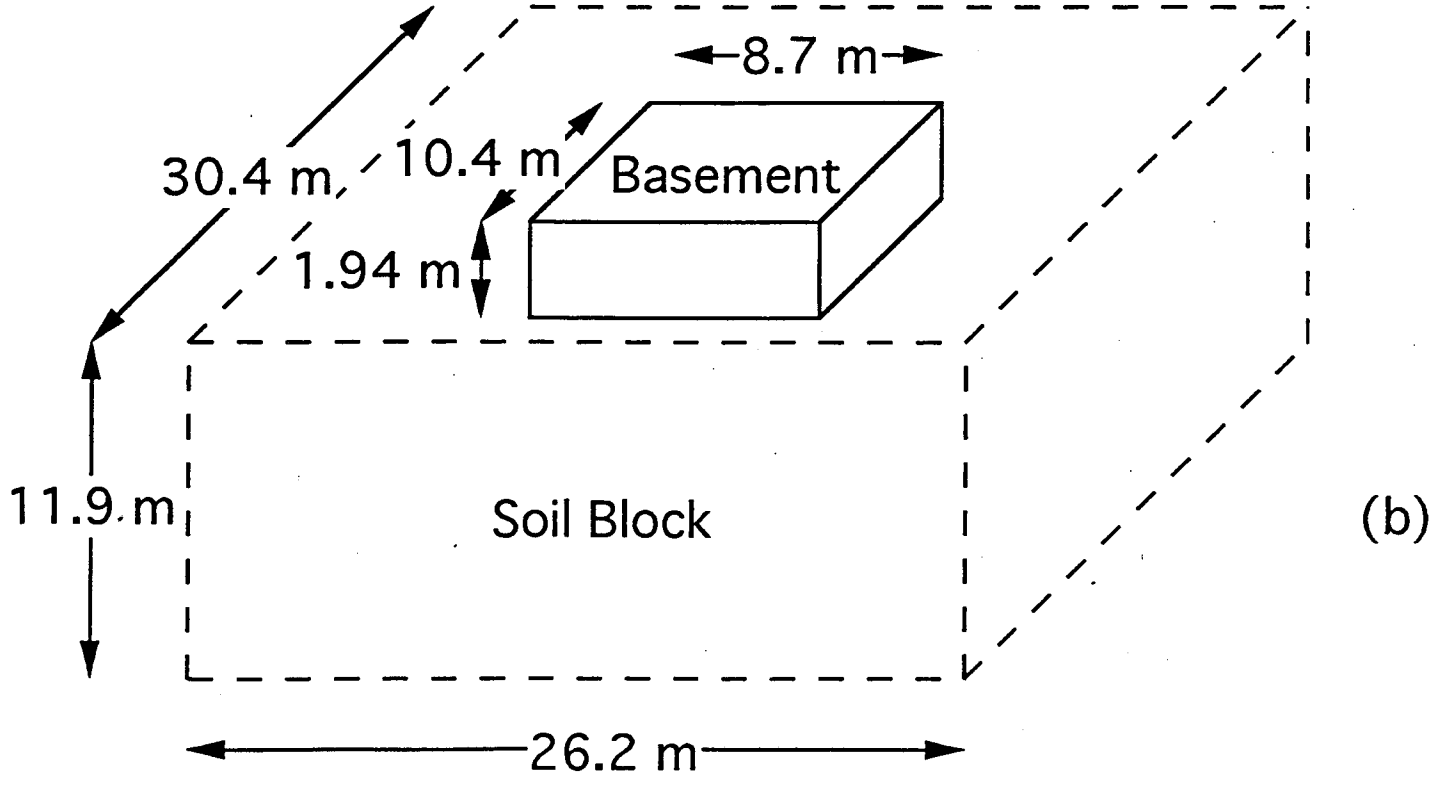
8.7 m
30.4 m
10.4 m
Basement
1.94 m
11.9 m
Soil Block
(b)
26.2 m

Figure 2

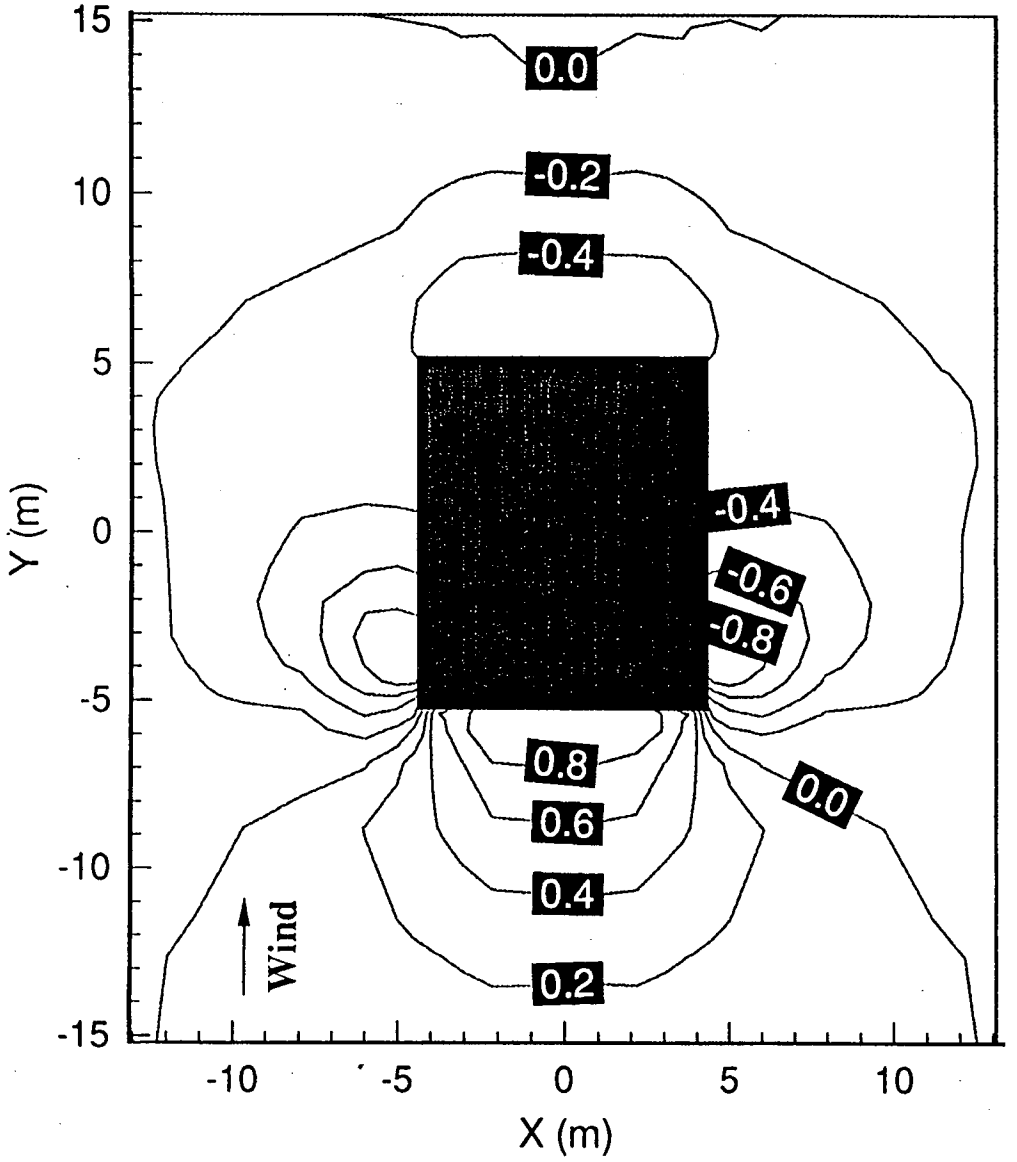

(a)

Figure 3a

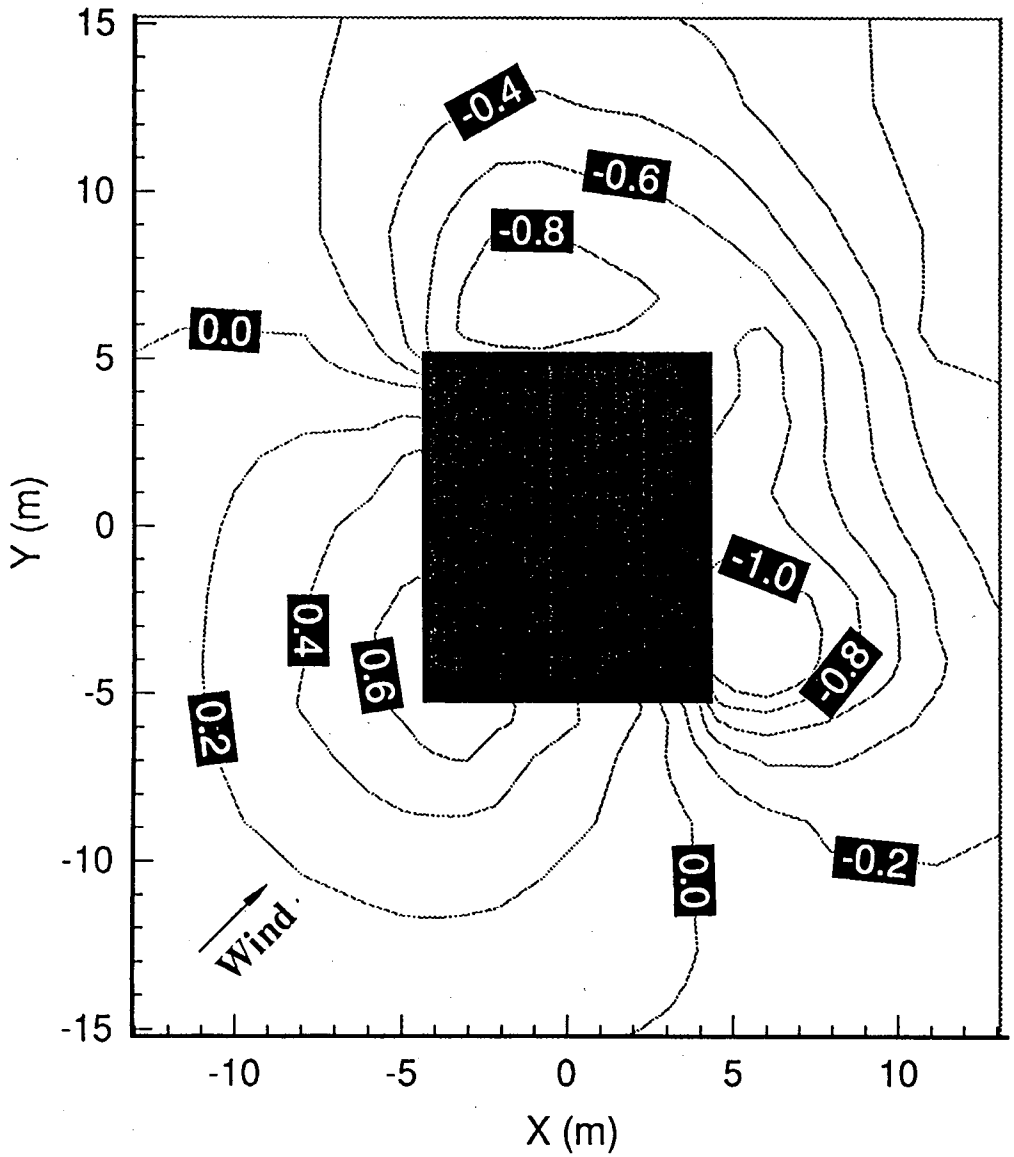

(b)

Figure 3b

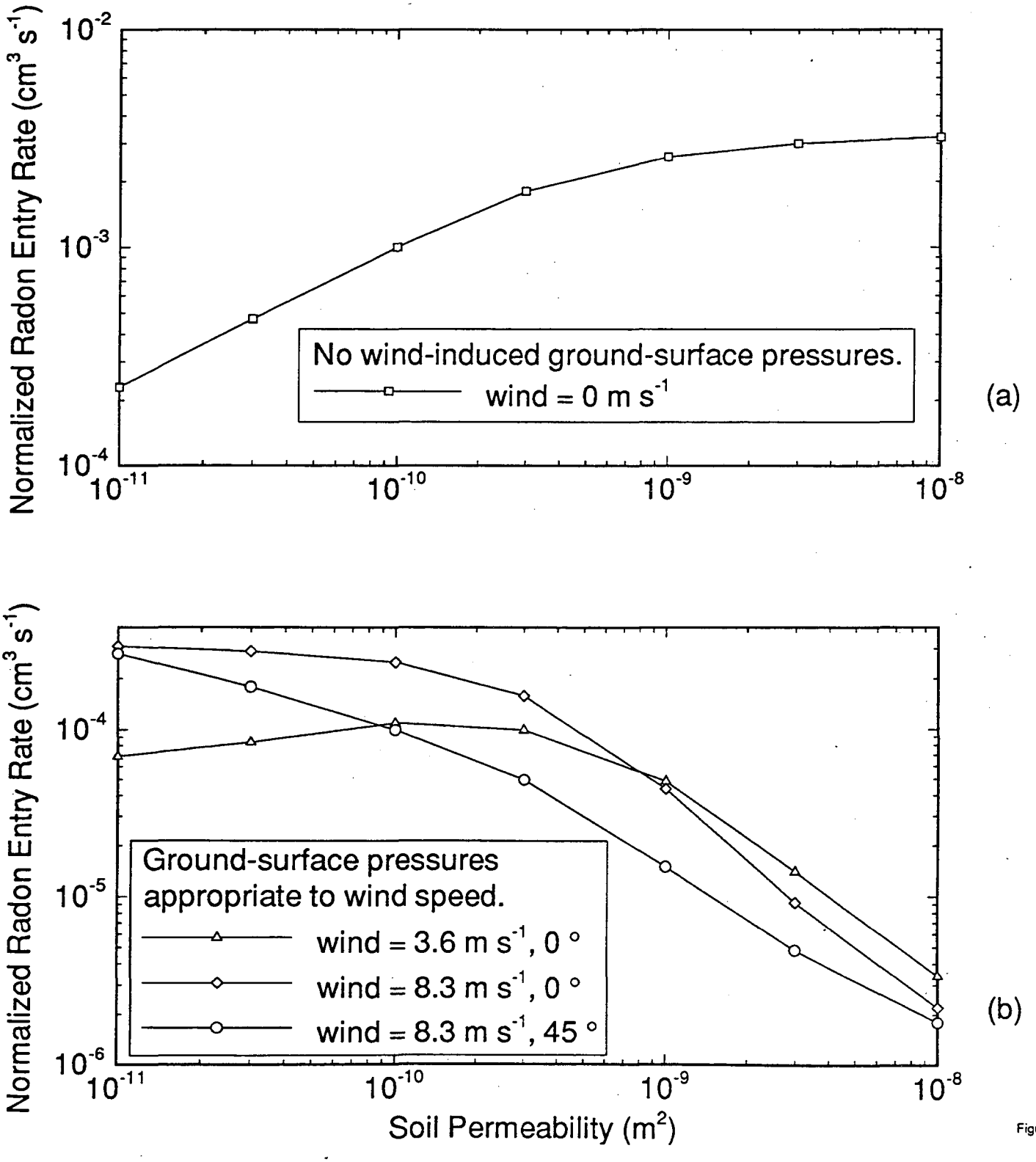
Normalized Radon Entry Rate (cm^3 s^{-1})
10^{-2}
10^{-3}
10^{-4}
10^{-11}
10^{-10}
10^{-9}
10^{-8}
No wind-induced ground-surface pressures.
wind = 0 m s^{-1}
(a)
Normalized Radon Entry Rate (cm^3 s^{-1})
10^{-4}
10^{-5}
10^{-6}
Ground-surface pressures
appropriate to wind speed.
wind = 3.6 m s^{-1}, 0 °
wind = 8.3 m s^{-1}, 0 °
wind = 8.3 m s^{-1}, 45 °
(b)
Soil Permeability (m^2)

Figure 4

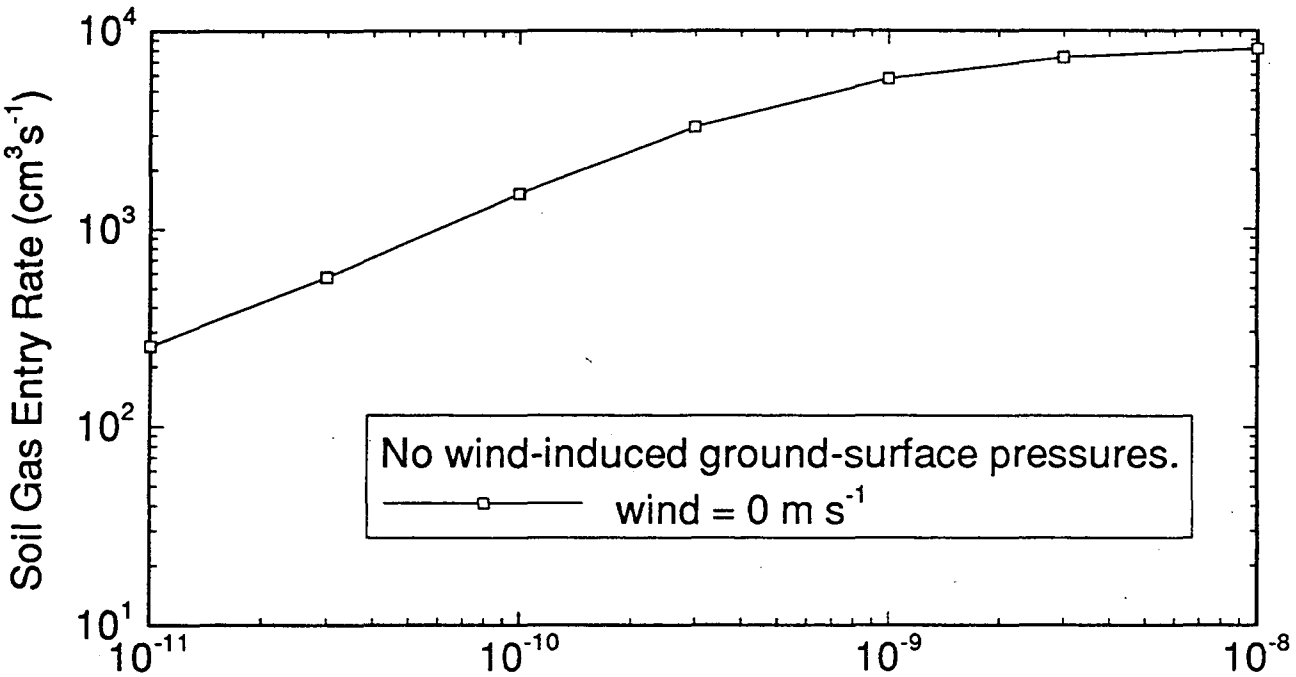
Soil Gas Entry Rate ($cm^3 s^{-1}$)
10^4
10^3
10^2
10^1
10^{-11}
10^{-10}
10^{-9}
10^{-8}
No wind-induced ground-surface pressures.
wind = 0 m s^{-1}

(a)

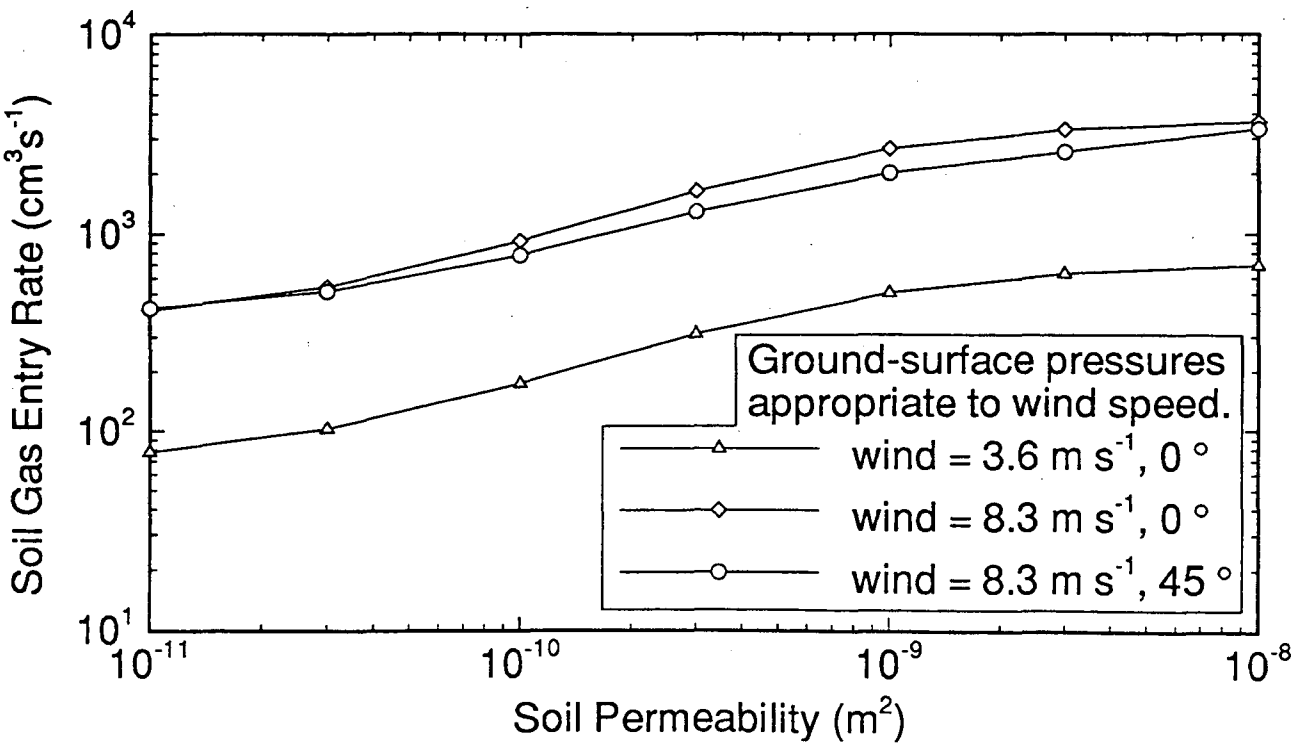
Soil Gas Entry Rate ($cm^3 s^{-1}$)
10^4
10^3
10^2
10^1
10^{-11}
10^{-10}
10^{-9}
10^{-8}
Soil Permeability (m^2)
Ground-surface pressures appropriate to wind speed.
wind = 3.6 m s^{-1}, 0 °
wind = 8.3 m s^{-1}, 0 °
wind = 8.3 m s^{-1}, 45 °

(b)

Figure 5

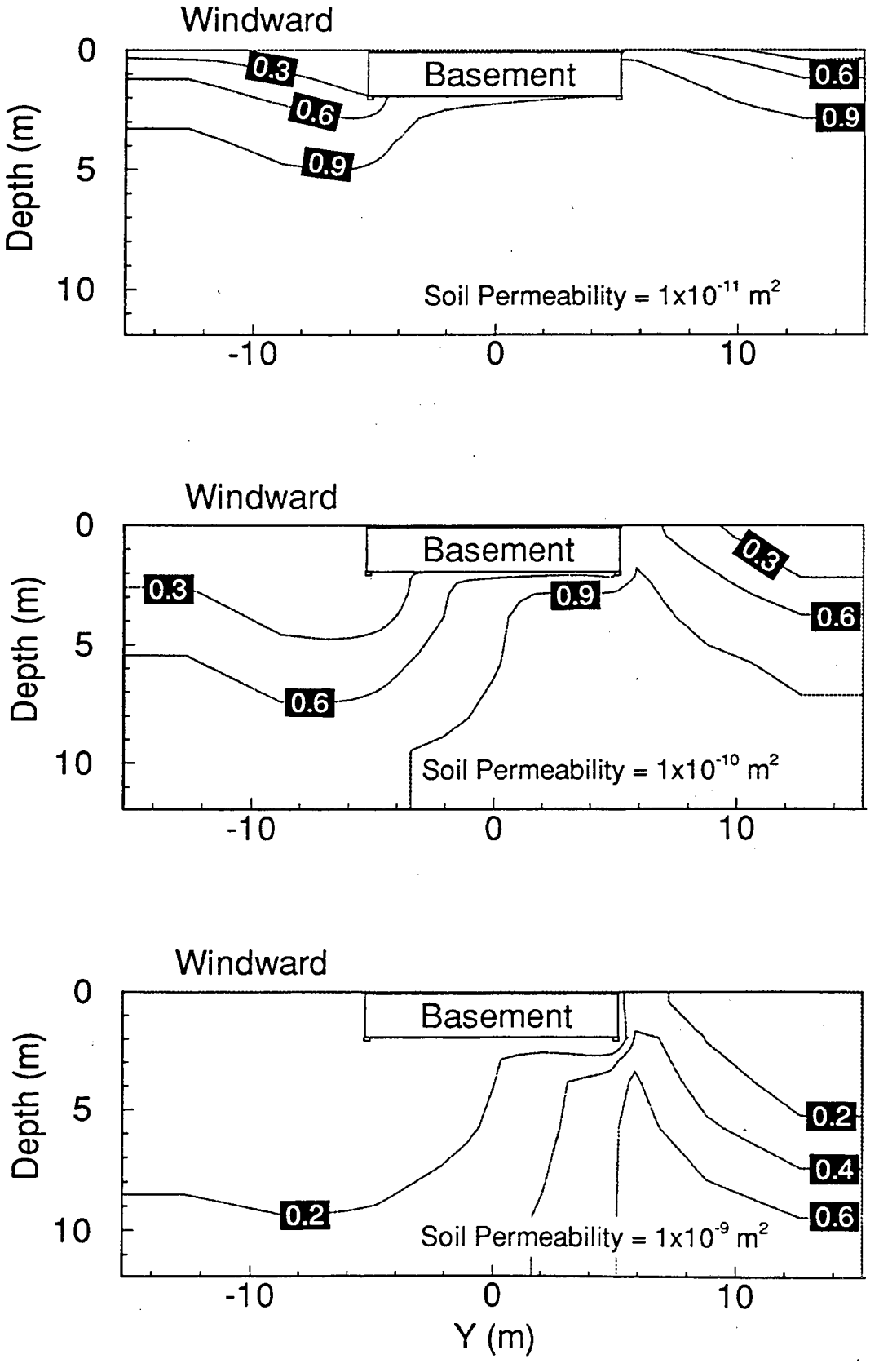
Windward
Basement
0.3
0.6
0.9
0.6
0.9
Depth (m)
0
5
10
Soil Permeability = 1x10^{-11} m^2
-10
0
10
Windward
Basement
0.3
0.9
0.3
0.6
0.6
Depth (m)
0
5
10
Soil Permeability = 1x10^{-10} m^2
-10
0
10
Windward
Basement
0.2
0.4
0.6
0.2
Depth (m)
0
5
10
Soil Permeability = 1x10^{-9} m^2
-10
0
10
Y (m)

(a)

Figure 6a

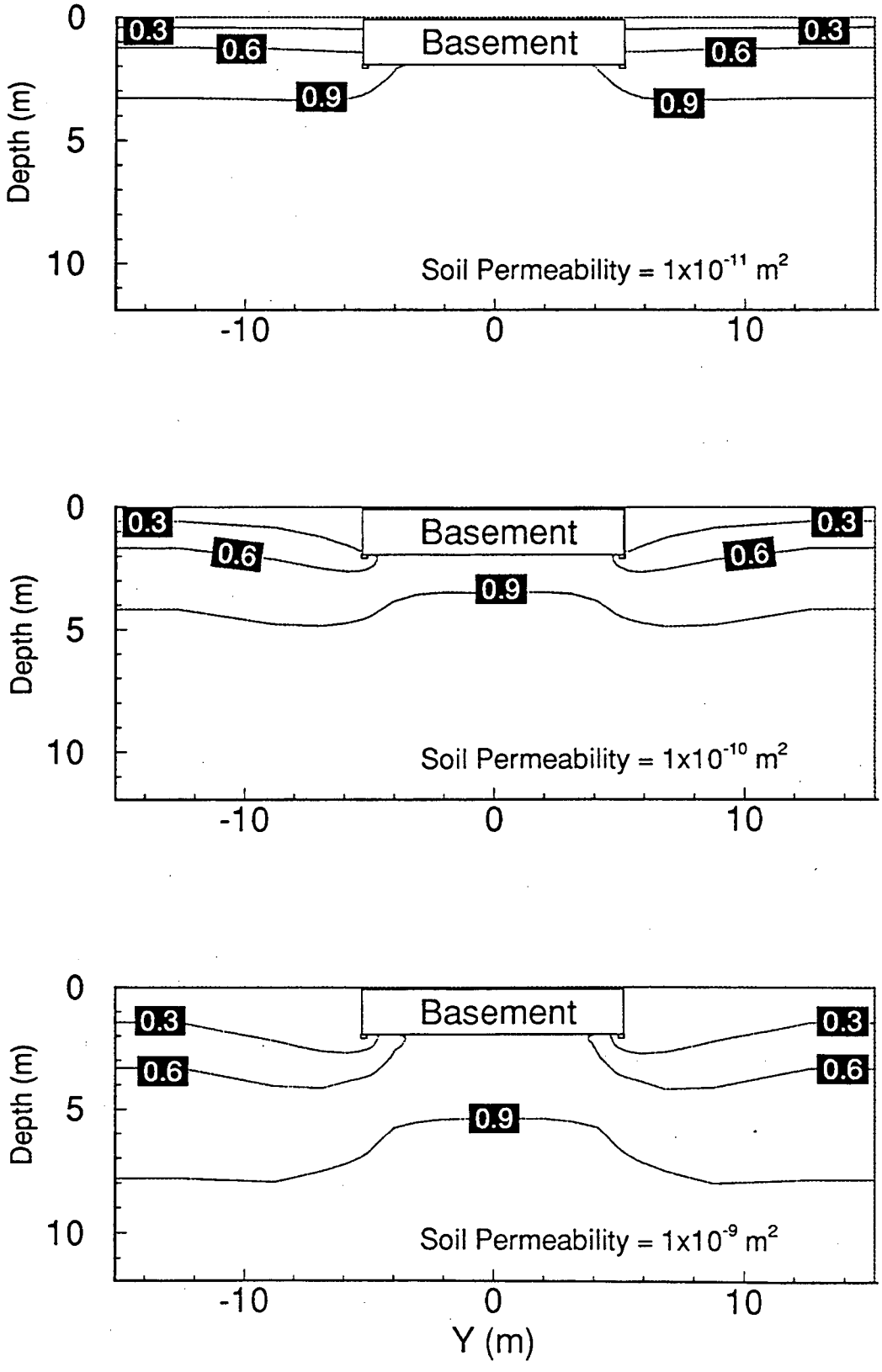
0
5
10
Depth (m)
0.3
0.6
0.9
Basement
Soil Permeability = 1x10^{-11} m^2
Soil Permeability = 1x10^{-10} m^2
Soil Permeability = 1x10^{-9} m^2
-10
0
10
Y (m)

(b)

Figure 6b

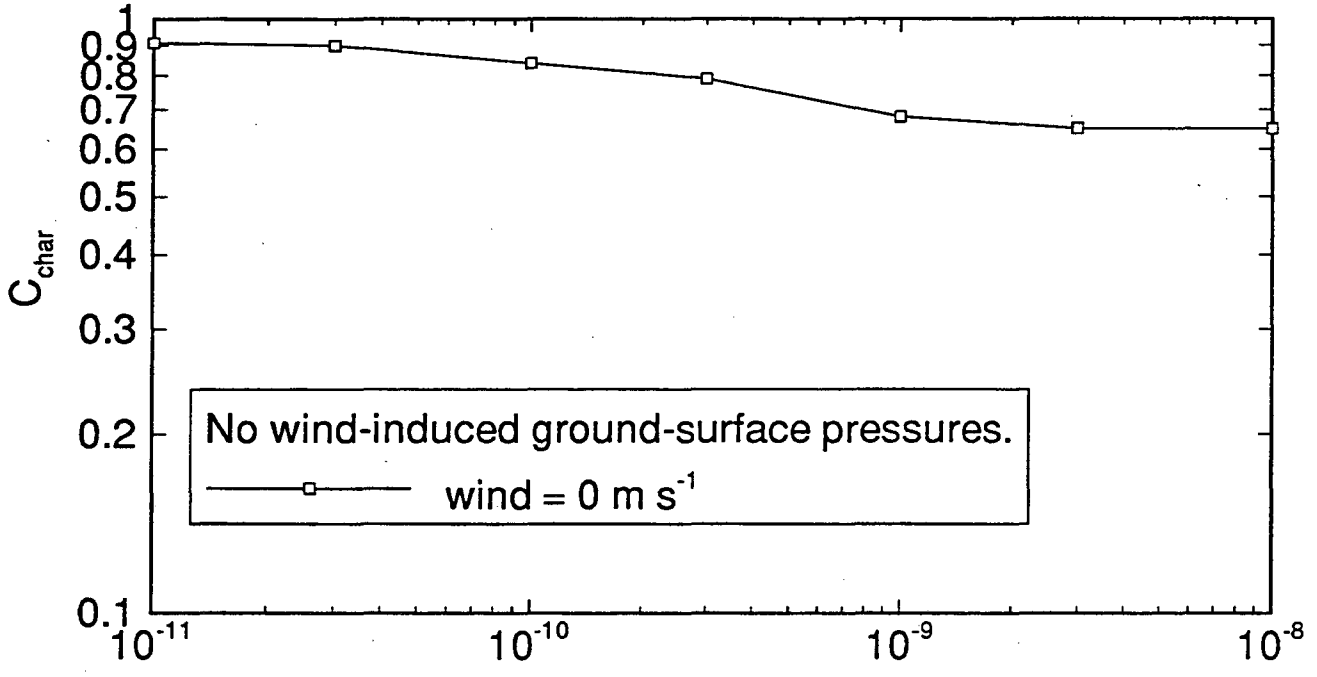
1
0.9
0.8
0.7
0.6
0.5
0.4
0.3
0.2
0.1
C_{char}
No wind-induced ground-surface pressures.
wind = 0 m s^{-1}
10^{-11}
10^{-10}
10^{-9}
10^{-8}

(a)

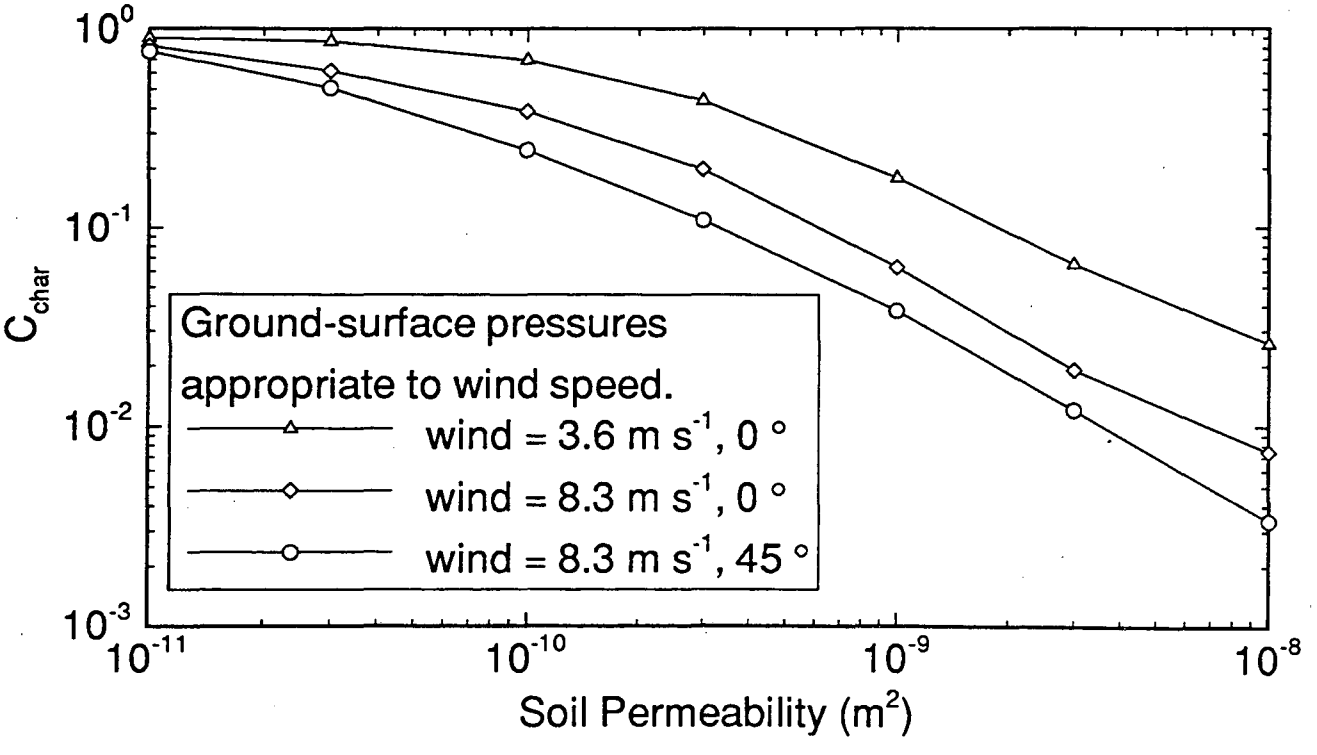
10^{0}
10^{-1}
10^{-2}
10^{-3}
C_{char}
Ground-surface pressures
appropriate to wind speed.
wind = 3.6 m s^{-1}, 0 °
wind = 8.3 m s^{-1}, 0 °
wind = 8.3 m s^{-1}, 45 °
10^{-11}
10^{-10}
10^{-9}
10^{-8}
Soil Permeability (m^2)

(b)

Figure 7

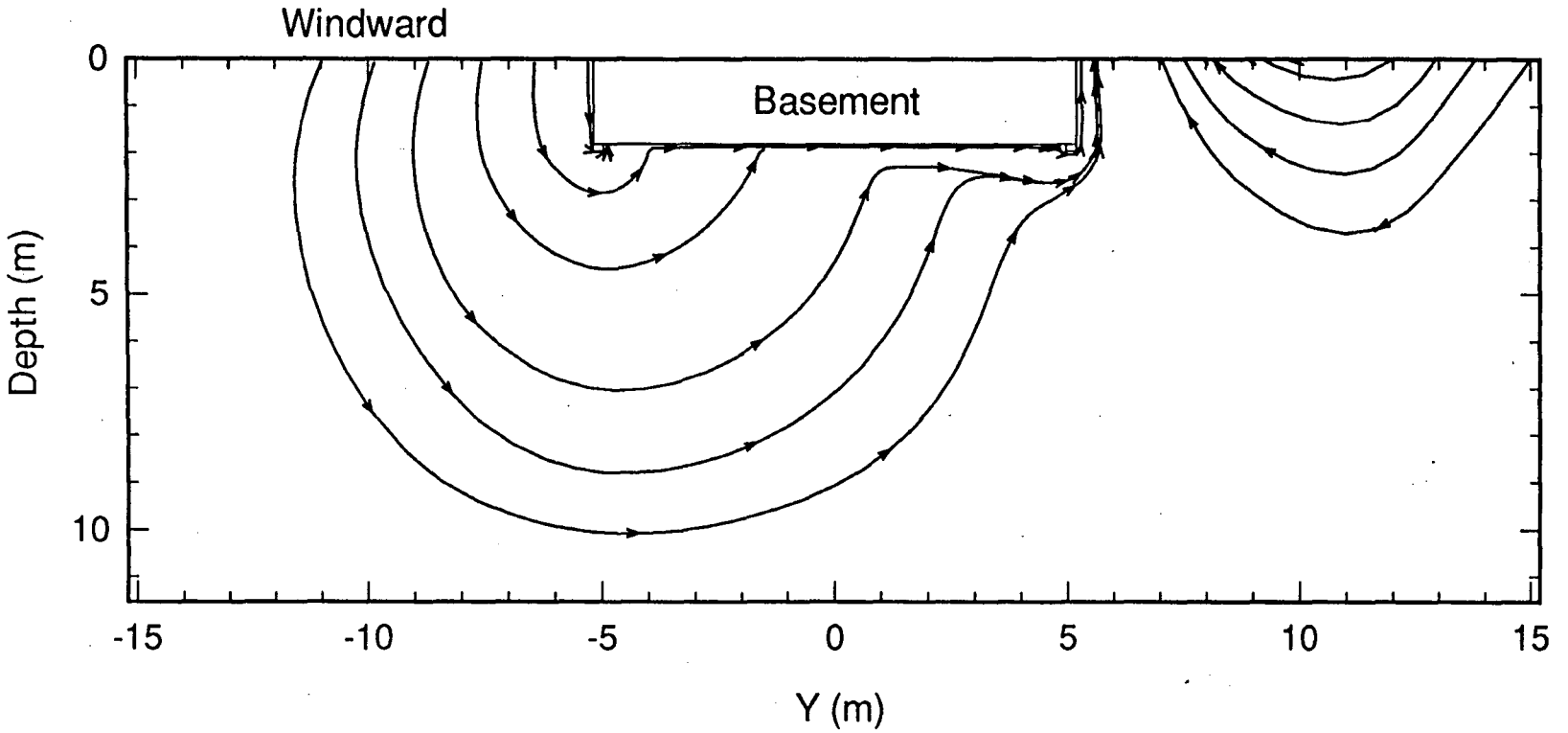

Figure 8

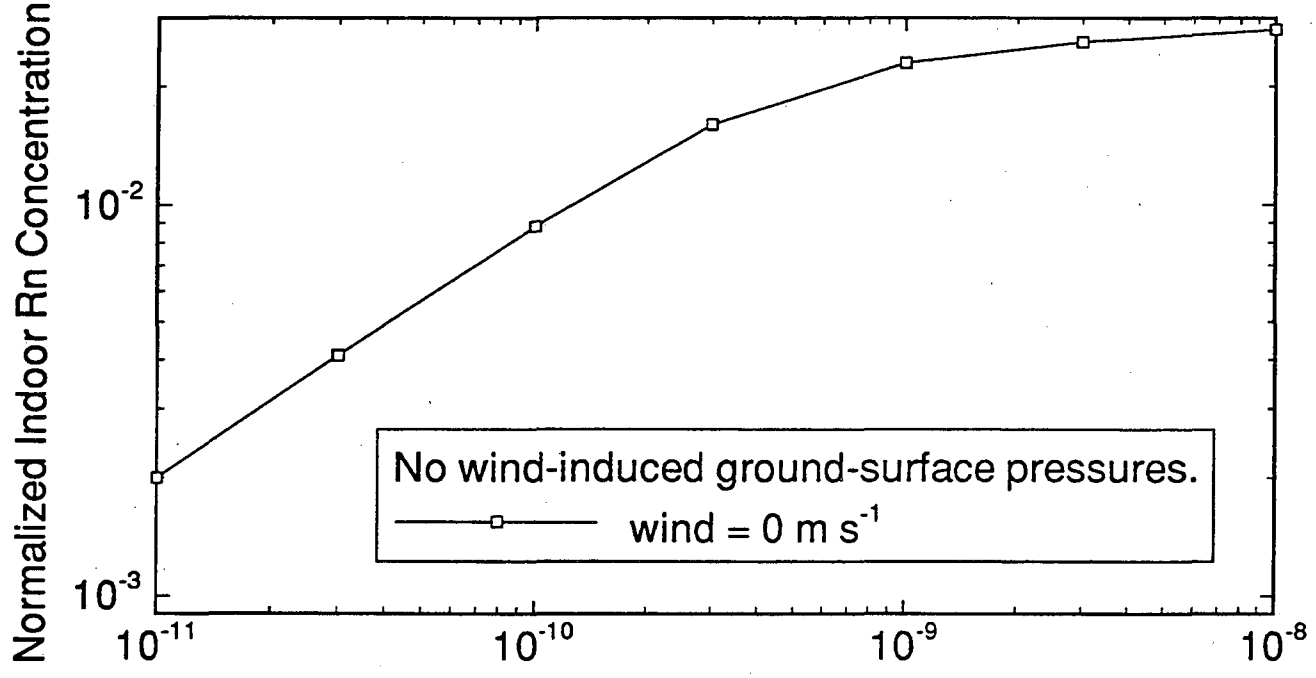
Normalized Indoor Rn Concentration
10^{-2}
10^{-3}
10^{-11}
10^{-10}
10^{-9}
10^{-8}
No wind-induced ground-surface pressures.
wind = 0 m s^{-1}

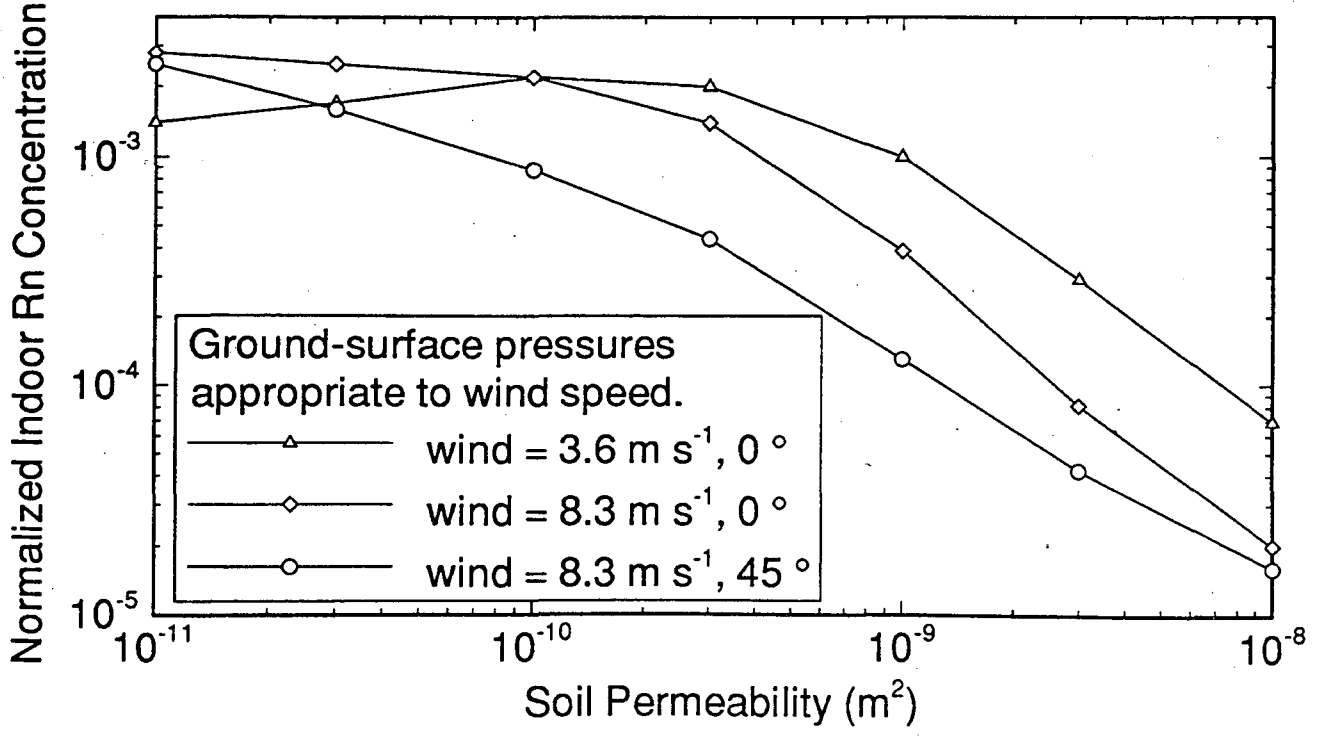
Normalized Indoor Rn Concentration
10^{-3}
10^{-4}
10^{-5}
10^{-11}
10^{-10}
10^{-9}
10^{-8}
Ground-surface pressures
appropriate to wind speed.
wind = 3.6 m s^{-1}, 0 °
wind = 8.3 m s^{-1}, 0 °
wind = 8.3 m s^{-1}, 45 °
Soil Permeability (m^2)

Figure 9

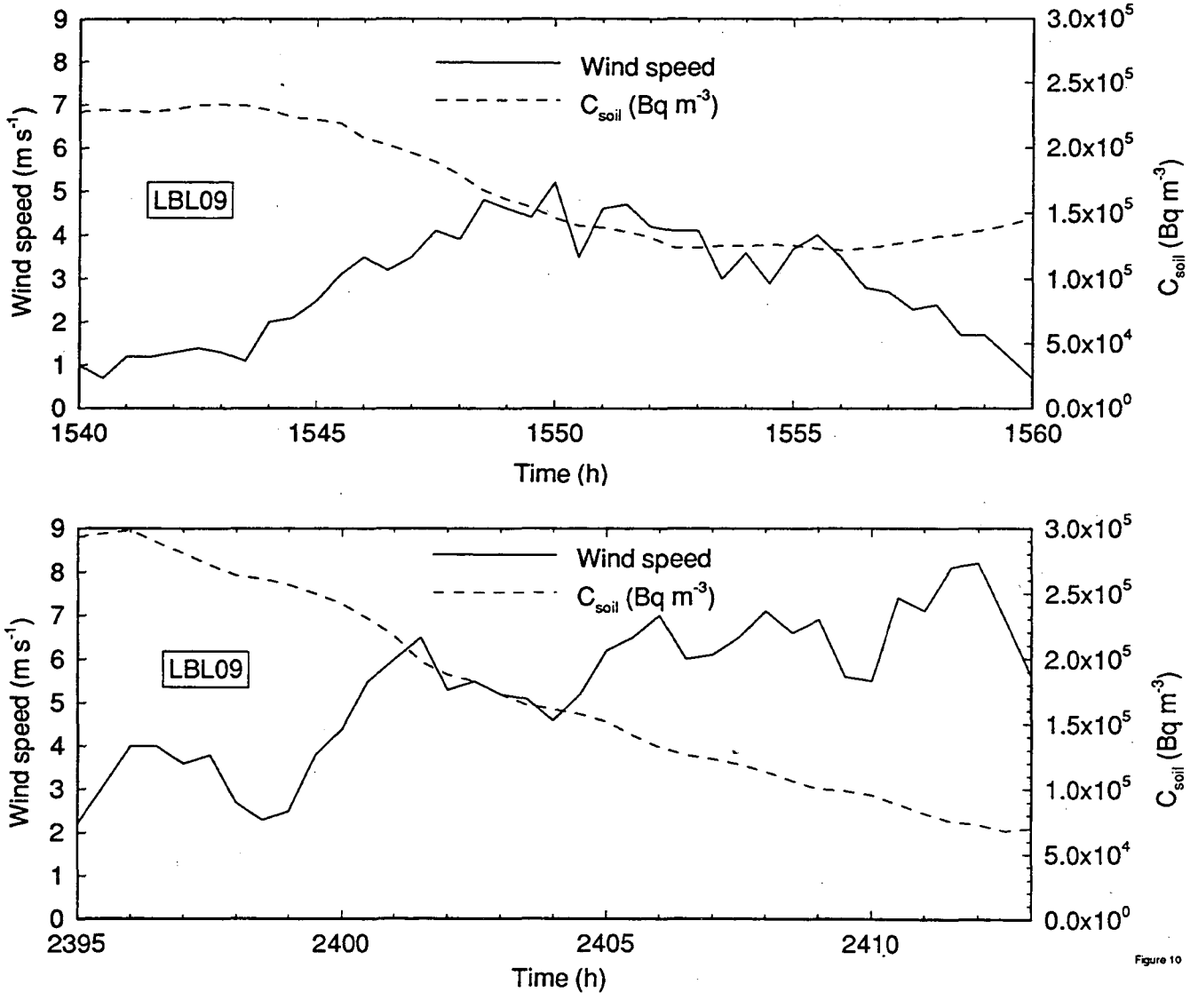
Wind speed
C_{soil} (Bq m^{-3})
LBL09
Wind speed (m s^{-1})
C_{soil} (Bq m^{-3})
Time (h)
0
1
2
3
4
5
6
7
8
9
1540
1545
1550
1555
1560
$0.0x10^0$
$5.0x10^4$
$1.0x10^5$
$1.5x10^5$
$2.0x10^5$
$2.5x10^5$
$3.0x10^5$
2395
2400
2405
2410

Figure 10

Table 1. Wind conditions, basement depressurization, and air exchange rate for the four simulation cases.

Case	*Wind Conditions*	*Basement Depressurization (Pa)*	*Air Exchange Rate (h^{-1})*	*Wind-induced ground-surface pressures*
1	none	-10.6	1.5	no
2	8.3 m s^{-1} at 0°	-10.6	1.5	yes
3	8.3 m s^{-1} at 45°	-10.6	1.5	yes
4	3.6 m s^{-1} at 0°	-2.00	0.65	yes

Table 2. Change in soil-gas radon concentration as a result of wind. Data culled from the LBL study of houses in New Jersey, reported in Turk et al., (1991).

House ID	Low Wind				High Wind				*Ratio*[b]
	Date	*Beginning Time*[a]	*Mean Wind* (m s^{-1})	*Mean Soil-Gas concentration* (kBq m^{-3})	*Date*	*Beginning Time*[a]	*Mean Wind* (m s^{-1})	*Mean Soil-Gas concentration* (kBq m^{-3})	
LBL09	22 Nov. 1986	1900	0.3	300	23 Nov. 1986	0200	3.5	220	0.7
	24 Nov. 1986	0400	1.3	240	24 Nov. 1986	1300	4.6	150	0.6
	28 Nov. 1986	1900	3.6	290	29 Nov. 1986	0100	8.2	74	0.3
LBL10	9 Jan. 1987	1700	1.7	380	10 Jan. 1987	0300	5.1	150	0.4
	27 Jan. 1987	0400	3.4	290	27 Jan. 1987	1400	6.8	160	0.6
LBL14	29 Nov. 1986	0900	2.6	81	29 Nov. 1986	1400	5.5	160	2
	12 Dec. 1986	0800	3.2	93	12 Dec. 1986	1200	10	56	0.6
	16 Dec. 1986	1800	0.9	100	17 Dec. 1986	0600	6.2	54	0.5
	21 Jan. 1987	0900	1.7	100	21 Jan. 1987	1600	8.2	44	0.4
	24 Jan. 1987	1700	4.8	140	25 Jan. 1987	0200	9.8	15	0.1

[a] Beginning of two-hour averaging period.
[b] Ratio of mean soil-gas concentration under high-wind conditions to that under low-wind conditions.

REFERENCES

Arnold L. J. (1990) A scale model study of the effects of meteorological, soil, and house parameters on soil gas pressures. *Health Physics*, 58, 559-573.

Baker P. H., Sharples S. and Ward I. C. (1987) Air flow through cracks. *Building and Environment*, 22 no. 4, 293-304.

Bauman F. S., Ernest D. R. and Arens E. A. (1988) ASEAN natural ventilation study: Wind pressure distributions on long building rows in urban surroundings. CEDR-03-88, Center for Environmental Design Research, University of California, Berkeley, CA.

Bonnefous Y. C. , Gadgil A. J., Fisk W. J., Prill R. J. and Nematollahi A. R. (1992) Field study and numerical simulation of subslab ventilation systems. *Environmental Science and Technology*, **26**, no. 9, 1752-1759.

Feustel H. E. (1985) Development of a simplified multizone infiltration model. LBL-19005, Lawrence Berkeley Laboratory, Berkeley, CA.

Fisk W. J., Prill R. J., Wooley J., Bonnefous Y. C., Gadgil A. J. and Riley W. J. (1994) New methods of energy efficient radon mitigation. To be submitted to *Energy and Buildings*.

FLUENT (1993) v4.2, Fluent Incorporated, Centerra Resource Park, 10 Cavendish Court, Lebanon, NH 03766.

Gadgil A. J., Bonnefous Y. C., Fisk W. J., Prill R. J. and Nematollahi A. (1991) Influence of subslab aggregate permeability on SSV performance. LBL-31160, Lawrence Berkeley Laboratory, CA.

Mowris R. J. and Fisk W. J. (1988) Modeling the effects of exhaust ventilation on ^{222}Rn entry rates and indoor ^{222}Rn concentrations. *Health Physics*, **54** No. 5, 491-501.

Nazaroff W. W., Feustel H., Nero A. V., Revzan K. L. and Grimsrud D. T. (1985) Radon transport into a detached one-story house with a basement. *Atmospheric Environment*, **19**, 31-46.

Nazaroff W. W., Moed B. A. and Sextro R. G. (1988) Soil as a source of indoor radon: generation, migration, and entry. In Nazaroff W. W. and Nero A. V. (Ed.) *Radon and its Decay Products in Indoor Air*, John Wiley, New York, 57-112.

Nazaroff W. W. (1992) Radon transport from soil to air. *Review of Geophysics*, **30**, 2, 137-160.

NOAA, National Oceanic and Atmospheric Administration (1980) Local climatological data, annual summaries for 1980, Part II - NEB - WYO, National Climatic Center, Asheville, NC 28801.

Owczarski P. C., Holford D. J., Burk K. W., Freeman H. D. and Gee G. W. (1991) Effect of winds in reducing sub-slab radon concentrations under houses laid over gravel beds. The 1991 International Symposium on Radon and Radon Reduction Technology: Volume 3, Philadelphia, PA, USEPA, Air and Energy Environmental Research Laboratory, Research Triangle Park, NC 27711.

Palmiter L. and Brown I. (1989) Northwest residential infiltration study, volume I: analysis and results. Prepared for the Bonneville Power Admin. (U.S. Dept. of Energy), DOE/BP-34625-1.

Patankar S. V. (1980) *Numerical Heat Transfer and Fluid Flow*. Hemisphere Publishing, New York.

Revzan K. L. and Fisk W. J. (1992) Modeling radon entry into houses with basements: The influence of structural factors. *Indoor Air*, **2**, 40-48.

Riley W. J., Gadgil A. J. and Nazaroff W. W. (1994) Wind-induced ground-surface pressures around a single family house. To be submitted to *J. Wind Eng. Ind. Aerodyn.*

Scott A. G. (1985) A computer model study of soil gas movement into buildings. Report No. 1389/1333, Department of Health and Welfare, Ottawa, Ontario, Canada.

Sherman M. H., Wilson D. J. and Kiel D. E. (1984) Variability in residential air leakage. Proc. Symposium on Measured Air Leakage Performance of Buildings, Philadelphia, PA: The American Society for Testing and Materials.

Sherman M. H. (1992) Simplified modeling for infiltration and radon entry. LBL-31305, Lawrence Berkeley Laboratory, Berkeley, CA.

Turk B.H., Prill R. J., Grimsrud D. T., Moed B. A and Sextro R. G. (1990) Characterizing the occurrence, sources, and variability of radon in Pacific northwest homes. *J. Air Waste Management Association*, **40**, 498-506.

Turk B. H., Harrison J. and Sextro R. G. (1991) Performance of radon control systems. *Energy and Buildings*, **17**, 157-175.

Van der Hoven I. (1957) Power spectrum of horizontal wind speed in the frequency range from 0.0007 to 900 cycles per hour. *J. Meteor.*, **14**, 160.

Ward D. C., Borak T. B. and Gadd M. S. (1993) Characterization of ^{222}Rn entry into a basement structure surrounded by low permeability soil. *Health Physics*, **65**, 1-11.

LAWRENCE BERKELEY LABORATORY
UNIVERSITY OF CALIFORNIA
TECHNICAL INFORMATION DEPARTMENT
BERKELEY, CALIFORNIA 94720